Proceedings of the ASME 2015 Dynamic Systems and Control Conference
DSCC2015
October 28-30, 2015, Columbus, Ohio, USA

DSCC2015-9718

ACCELERATED EVALUATION OF AUTOMATED VEHICLES IN LANE CHANGE SCENARIOS

Ding Zhao
Huei Peng
Dept. of Mechanical Engineering
University of Michigan
Ann Arbor, MI, USA

Henry Lam
Dept. of Industrial and Operations Engineering
University of Michigan
Ann Arbor, MI, USA

Shan Bao
Kazutoshi Nobukawa
David J. LeBlanc
University of Michigan Transportation Research Institute
Ann Arbor, MI, USA

Christopher S. Pan
Division of Safety Research, NIOSH, CDC
Morgantown, WV, USA

ABSTRACT

It is important to rigorously and comprehensively evaluate the safety of Automated Vehicles (AVs) before their production and deployment. A popular AV evaluation approach is Naturalistic-Field Operational Test (N-FOT) which tests prototype vehicles directly on public roads. Due to the low exposure to safety-critical scenarios, N-FOTs is time-consuming and expensive to conduct. Computer simulations can be used as an alternative to N-FOTs, especially in terms of generating motions of the surrounding traffic. In this paper, we propose an accelerated evaluation approach for AVs. Human-controlled vehicles (HVs) were modeled as disturbance to AVs based on data extracted from the Safety Pilot Model Deployment Program. The cut-in scenarios are generated based on skewed statistics of collected human driver behavior, which amplifies riskier testing scenarios while reserves its statistical information so that the safety benefits of AV in non-accelerated cases can be accurately estimated. An AV model based on a production vehicle was tested. Results show that the proposed method can accelerate the evaluation process by at least 100 times.

INTRODUCTION

AV technologies are actively studied by many automotive companies because of their potential to save fuel, reduce crashes, ease traffic congestion, and provide better mobility to the population that could not operate a car [1]. Currently, almost all major automakers have research and development programs on AVs. In 2030, it is estimated that the sales of AV technologies may reach $87 billion [2].

AVs will penetrate the market gradually and will co-exist with non-AVs for decades. During this transition period, AVs will interact mostly with HVs. It is estimated that 70-90% of the motor vehicle crashes are due to human errors [3], [4]. To reduce crashes, AVs must deal with the imperfect maneuvers initiated by human drivers. A practical and effective evaluation approach that accounts for imperfect human driven traffic is essential for the development and evaluation of AVs.

One approach to study the interactions between AVs and HVs is through Naturalistic Field Operational Tests (N-FOT) [5]. In an N-FOT, data is collected from a number of equipped vehicles driven under naturalistic conditions over an extended period of time [6]. Several N-FOT projects [7]–[15] have been conducted in the U.S. and Europe. Conducting an N-FOT to evaluate an AV function typically involves non-intrusive conditions, i.e., the test drivers were told to drive as they normally would on public roads. This test approach suffers several limitations. An obvious problem is the time needed. Under naturalistic conditions, the level of exposure to dangerous events is very low. In the U.S., there were 5,615,000 police-reported motor vehicle crashes and 30,800 fatal crashes in 2012, while the vehicles traveled a total of 2,968 billion miles [16]. This translates to approx. 0.53 million miles for each police-reported crash and 96 million miles for a fatal crash. Since the average annual mileage driven by licensed drivers is 14,012 miles, one needs to drive on average 38 years to be involved in a police-reported crash and 6,877 years for a fatal crash. Because of this low exposure rate, the N-FOT projects need a large number of vehicles, long test duration, and a large budget.

According to [17], N-FOT projects "cannot be conducted with less than $10,000,000". It should be noted that some researchers took advantage of big data from N-FOTs and applied N-FOT data in a simulation environment [18], [19]. Reusing the N-FOT data in simulations is a good approach to testing various designs to avoid the large budget for FOT. However, even for computer simulations, low exposure to safety critical scenarios is still an issue.

The test matrix approach has been the basis of many test standards, such as AEB (Autonomous Emergency Braking) test protocol [20] of the Euro NCAP (New Car Assessment Program). Much development work was done to advance this evaluation approach including CAMP [21], HASTE [22], AIDE [23], TRACE [24], APROSYS [25], ASSESS [26], etc. The test scenarios are frequently selected based on national crash databases [27], such as GES (General Estimates System) [28], NMVCCS (National Motor Vehicle Crash Causation Survey) [29] and EDR (Event Data Recorder databases) [30]. The main benefits of these test methods are that they are clearly defined, repeatable, reliable, and can be finished in a reasonable amount of time. However, it is not trivial to choose and reconstruct test scenarios to represent real-world conditions [6], [31], especially when human interaction is involved. Moreover, because all the test scenarios are fixed and predefined, control systems can be adjusted to achieve good performance on these tests, but their behaviors under broader conditions are not adequately assessed [32].

Another approach, the Worst-Case Scenario Evaluation (WCSE) methodology has been studied by Ma [33], Ungoren [34] and Kou [35] to identify the most challenging scenarios based on the analysis of vehicle dynamics and control. While the worst-case evaluation method can identify the weakness of a vehicle and vehicle control systems, it did not consider the probability of such worst-case scenarios. Therefore, the worst case evaluation results do not provide sufficient information about the risk in real world [36], [37], and may not be the fairest way to compare different designs.

Zhao [38] proposed the concept of accelerated evaluation of AV and applied this approach to car-following scenarios. The dynamics of the lead vehicle was exemplified to generate a riskier conditions for the following AVs. The acceleration rate was estimated by comparing the crash rate under accelerated conditions and naturalistic conditions for human driven vehicles. The proposed approach is useful to compare between AV designs, but not yet able to rigorously estimate the crash rate of a new AV under naturalistic conditions and evaluate its safety benefit.

In this paper, we propose a new approach of accelerated evaluation that can be used to estimate real world safety benefits by using the importance sampling techniques. First, HVs are modeled based on data extract from N-FOT database with stochastic variables to represent the human driving behaviors. Second, the HV models are modified using importance sampling, which makes the drivers act more aggressively and thus could generate safety critical scenarios at a higher frequency. The 'exemplified' results are then corrected to produce estimations statistically equivalent to the original naturalistic driving conditions. A concept AV algorithm is modeled and evaluated using the proposed approach in lane change scenarios.

MODEL OF THE LANE CHANGE SCENARIOS

The lane change (cut-in) scenario is used as an example to show the benefits of the proposed accelerated evaluation approach. In the US, there are between 240,000 and 610,000 reported lane-change crashes, resulting in 60,000 injuries annually [39]. Few protocols have been published regarding the evaluation of AVs (e.g., Autonomous emergency braking systems) under lane change scenarios.

Human drivers' lane change behaviors have been analyzed and modeled for more than half a century. Early studies based on controlled experiments usually have short test horizons and limited control settings [40]. More recently, researchers started to use large scale N-FOT databases to model the lane change behaviors. Lee [40] examined steering, turn signal and brake pedal usage, eye glance patterns, and safety envelope of 500 lane changes. The 100-Car Naturalistic Driving Study analyzed lane change events leading to rear-end crashes and near-crashes [39]. Zhao [41] analyzed the safety critical variables in mandatory and discretionary lane changes for heavy trucks [10]. Most of these studies are based on hundreds of lane changes. We use the data collected in the Safety Pilot Model Deployment project, which contains hundreds of thousands of lane changes.

Naturalistic lane change events

In this research, we developed a lane change statistical model and demonstrated its use for accelerated evaluation of a frontal collision avoidance algorithm. The database used is the Safety Pilot Model Deployment (SPMD) database [42]. The SPMD program aims to demonstrate connected vehicle technologies in a real-world environment. It recorded naturalistic driving of 2,842 equipped vehicles in Ann Arbor, Michigan for more than two years. As of April 2015, 34.9 million miles were logged, making SPMD one of the largest public N-FOT databases ever.

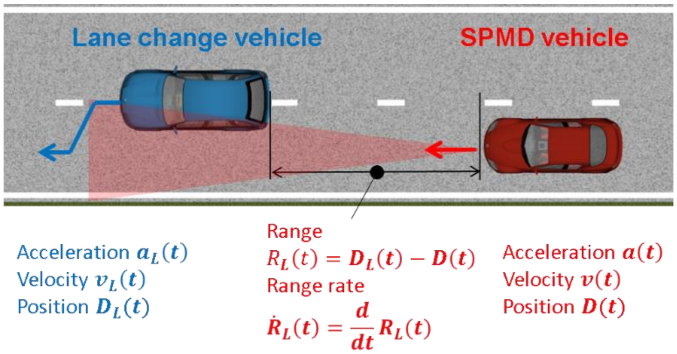

Fig. 1. Lane change scenarios that may cause frontal crashes

As shown in Fig. 1, a lane change was detected and recorded by a SPMD vehicle when the Lane Change Vehicle (LCV) crosses the lane markers. In the SPMD program, 98 sedans are equipped with Data Acquisition System with MobilEye® [43], which provides a) the relative position (range), and b) lane tracking measures pertaining to the lane delineation both from the painted boundary lines and road edge characteristics. The accuracy of MobilEye® for range and speed measurement was examined by comparing with a 77 GHz radar over 660 km (412 miles) of driving on a variety of road types, weather, and ambient light conditions. It was found that the MobilEye® provides measures similar to the radar when the range is shorter than 75 m.

The following criteria were applied to ensure consistency of the used dataset:

- $v(t_{LC}) \in (2\text{ m/s}, 40\text{ m/s})$
- $v_L(t_{LC}) \in (2\text{ m/s}, 40\text{ m/s})$
- $R_L(t_{LC}) \in (0.1\text{ m}, 75\text{ m})$

where t_{LC} is the time when the center line of the LCV crosses the lane markers; v_L and v are the velocities of the LCV and SPMD vehicle; R_L is the range, defined as the distance between the rear edge of the LCV and the front edge of the SPMD vehicle; TTC (Time To Collision) is defined as

$$TTC = -\frac{R_L}{\dot{R}_L} \tag{1}$$

where $\dot{R}_L$ is the derivative of R_L. 403,581 lane changes were detected. Fig. 2 shows the locations of the identified lane changes.

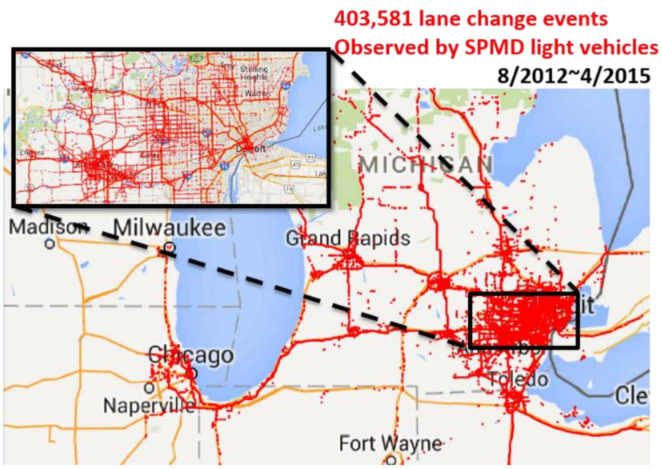

Fig. 2. Recorded lane change events queried from SPMD database

Lane change models

Generally, a lane change can be categorized into three phases: decision to initiate a lane change, gap (range) acceptance, and lane change execution [40]. In this research, we focused on the effects of gap acceptance, which is mainly captured by three variables: $v_L(t_{LC})$, $R_L(t_{LC})$ and $TTC_L(t_{LC})$. In the following contents, unless mentioned specifically, v_L, R_L and TTC_L are the values at t_{LC}.

The distribution of v_L is shown in Fig. 3. The division of highways and local roads is embodied by the bimodal shape of the histogram. v_L is assumed to remain constant during the execution of lane change. Only the events with negative range rate is used to build the lane change model. Out of 403,581 lane change events, 173,692 are with negative range rate.

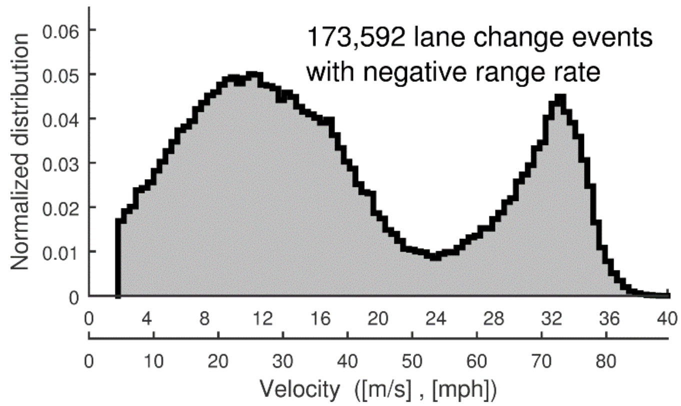

Fig. 3. Distributions of $v_L(t_{LC})$ of the lane change events used the our model

To capture the influence of vehicle speed on the range and TTC, we divided lane change events into low, medium and high velocity conditions. Fig. 4 shows that v_L has little influence on the distribution of R_L^{-1}. Fig. 5 illustrates the fitting of R_L^{-1} with Pareto distribution

$$f_{R_L^{-1}}\left(x \middle| k_{R_L^{-1}}, \sigma_{R_L^{-1}}, \theta_{R_L^{-1}}\right) = \frac{1}{\sigma_{R_L^{-1}}}\left(1 + k_{R_L^{-1}}\frac{x-\theta_{R_L^{-1}}}{\sigma_{R_L^{-1}}}\right)^{-1-1/k_{R_L^{-1}}} \tag{2}$$

where the shape parameter $k_{R_L^{-1}}$, the scale parameter $\sigma_{R_L^{-1}}$, and threshold parameter $\theta_{R_L^{-1}}$ are all positive.

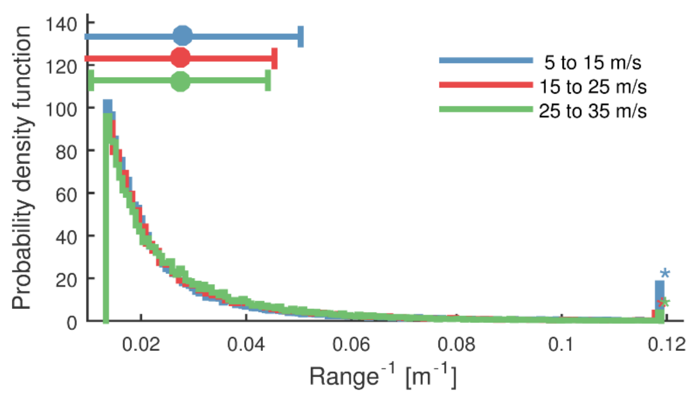

Fig. 4. Distributions of $R_L^{-1}(t_{LC})$ at different vehicle forward speeds

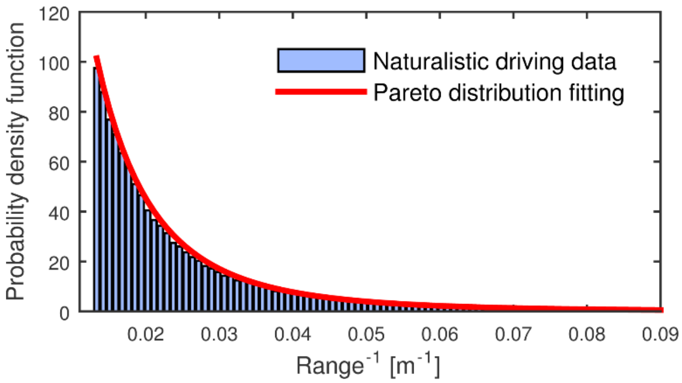

Fig. 5. Fitting results of $R_L^{-1}(t_{LC})$ using the Pareto distribution

The histograms of TTC_L^{-1} for different velocity intervals are shown in Fig. 6. As the vehicle speed increases, the mean of TTC_L^{-1} decreases. TTC_L^{-1} can be approximated by an exponential distributions

$$f_{TTC_L^{-1}}\left(x \middle| \lambda_{TTC_L^{-1}}\right) = \frac{1}{\lambda_{TTC_L^{-1}}} e^{-x/\lambda_{TTC_L^{-1}}} \tag{3}$$

where the scaling factor $\lambda_{TTC_L^{-1}}$ varies with the speed of the LCV.

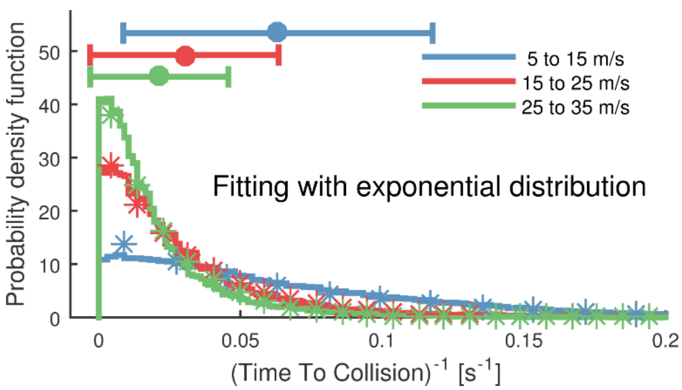

Fig. 6. Distribution of $TTC_L^{-1}(t_{LC})$ at different lane change vehicle speeds

The dependence of $\lambda_{TTC_L^{-1}}$ on vehicle speed is shown in Fig. 7. As vehicle speed increases, $\lambda_{TTC_L^{-1}}$ decreases. The blue circles represent $\lambda_{TTC_L^{-1}}$ at the center points of v_L intervals. We use linear interpolation and extrapolation to create smooth $\lambda_{TTC_L^{-1}}$ for all vehicle speeds.

The effect of range on TTC is shown in Fig. 8. It can be seen that the influence of range on TTC is very limited. This indicates that R_L and TTC_L can be modeled independently given the same v_L. $\dot{R}_L$ can then be calculated from

$$\dot{R}_L = -\frac{TTC_L^{-1}}{R_L^{-1}} \tag{4}$$

Finally, velocity of the host vehicle v at t_{LC} can be calculated from

$$v(t_{LC}) = v_L(t_{LC}) - \dot{R}_L(t_{LC}) \tag{5}$$

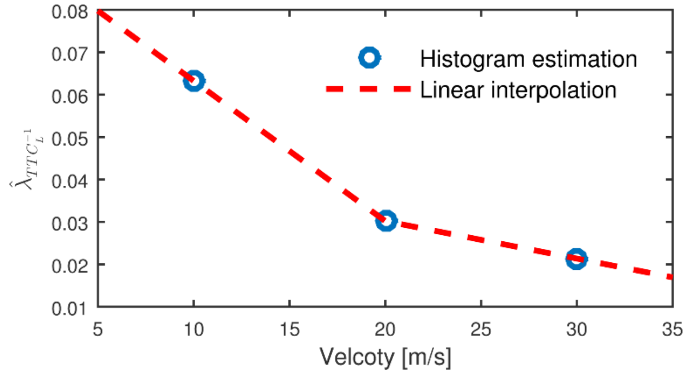

Fig. 7. Model parameters for $TTC_L(t_{LC})$

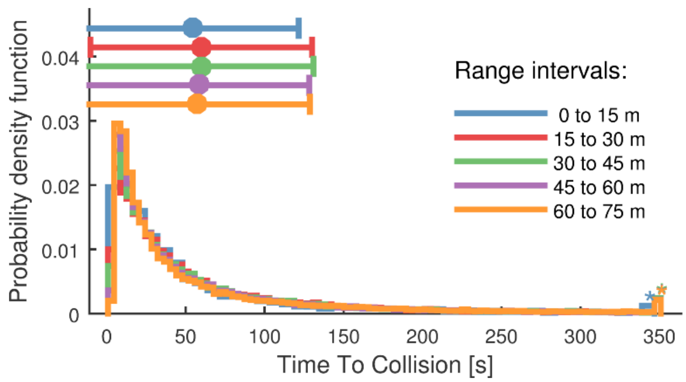

Fig. 8. Distribution of $TTC_L(t_{LC})$ with variant $R_L(t_{LC})$ intervals

In summary, the lane change events are generated in the following order: a) generate v_L based on the empirical distributions shown in Fig. 3; b) generate R_L^{-1} using Fig. 5; c) generate TTC_L^{-1} using the Exponential distribution with parameters shown in Fig. 7; d) calculate $v(t_{LC})$ using Eqs.(4) and (5).

ACCELERATED EVALUATION

Monte Carlo techniques can be used to simulate the driving conditions using the generated stochastic model, but a naïve implementation will take a long time to execute. The concept of accelerated evaluation is proposed to shorten the simulation time. In this section, we introduce the Importance Sampling (IS) concept and show how to apply IS to accelerate the evaluation process.

Importance Sampling

IS is based on the concept of variance reduction, which is effective in handling rare events. IS has been successfully applied to evaluate critical events in reliability [44], finance [45], insurance [46], and telecommunication networks [47]. General overviews can be found in [48]–[50].

To explain the concept of IS, let $\mathcal{E}$ be the rare events of interest, and in this paper, frontal crashes with a vehicle cutting in. The indicator function of the event $\mathcal{E}$ is defined as

$$I_{\mathcal{E}}(\boldsymbol{x}) = \begin{cases} 1, & if\ \boldsymbol{x} \in \mathcal{E} \\ 0, & otherwise \end{cases} \tag{6}$$

The random vector $\boldsymbol{x}$ represents the motions of the lane change vehicle. Our task is to estimate the probability of $\mathcal{E}$ happening, i.e.

$$\gamma \coloneqq \mathrm{P}(\mathcal{E}) = \mathrm{E}(I_{\mathcal{E}}(\boldsymbol{x})) \tag{7}$$

Denote $f(\boldsymbol{x})$ as the joint density function of $\boldsymbol{x}$. The core idea of IS is to replace $f(\boldsymbol{x})$ with a new IS density $f^*(\boldsymbol{x})$ that has a higher likelihood of the rare events. Obviously, using a different distribution like $f^*(\boldsymbol{x})$ leads to biased samples, and the key of IS is to provide a mechanism to compensate for this bias and computes correct crash rate at the end.

We describe this mechanism as follows. First, we define the so-called likelihood ratio L (Radon-Nikodym derivative [51]) as

$$L(x) = \frac{f(\boldsymbol{x})}{f^*(\boldsymbol{x})} \tag{8}$$

where $f(\boldsymbol{x})$ is the original probability distribution.

The probability of $\mathcal{E}$ satisfies

$$\begin{aligned} \mathrm{P}(\mathcal{E}) &= \mathrm{E}_f\big(I_{\mathcal{E}}(\boldsymbol{x})\big) \\ &= \int I_{\mathcal{E}}(\boldsymbol{x}) f(\boldsymbol{x}) d\boldsymbol{x} \\ &= \int [I_{\mathcal{E}}(\boldsymbol{x}) L(\boldsymbol{x})] f^*(\boldsymbol{x}) \mathrm{d}\boldsymbol{x} \\ &= \mathrm{E}_{f^*}(I_{\mathcal{E}}(\boldsymbol{x}) L(\boldsymbol{x})) \end{aligned} \tag{9}$$

One required condition for (9) to hold is that $f^*(\boldsymbol{x})$ must be absolutely continuous with respect to $f(\boldsymbol{x})$ within $\mathcal{E}$, i.e.

$$\forall x \in \mathcal{E}: f^*(\boldsymbol{x}) = 0 \quad \Rightarrow \quad f(\boldsymbol{x}) = 0 \tag{10}$$

which guarantees the existence of L in (8). The IS sample is $I_{\mathcal{E}}(\boldsymbol{x}_i) L(\boldsymbol{x}_i)$ where $\boldsymbol{x}_i$ is generated under $f^*(\boldsymbol{x})$, which is an unbiased estimator for γ. The overall IS estimator for test number n is then

$$\hat{\gamma}_n = \frac{1}{n} \sum_{i=0}^{n} I_{\mathcal{E}}(\boldsymbol{x}_i) L(\boldsymbol{x}_i) \tag{11}$$

The accuracy of the estimation is represented by the relative half-width. With the Confidence level at $100(1-\alpha)$ %, the relative half-width of $\hat{\gamma}_n$ is defined as

$$l_r = \frac{l_\alpha}{\gamma} \tag{12}$$

where l_α is the half-width given by

$$l_\alpha = z_\alpha \sigma(\hat{\gamma}_n) \tag{13}$$

and z_α is defined as

$$z_\alpha = \Phi^{-1}(1 - \alpha/2) \tag{14}$$

where Φ^{-1} is the inverse cumulative distribution function of $\mathcal{N}(0,1)$. Given that the requirement for estimation accuracy is to make l_r smaller than a constant β, under accelerated evaluation, it can be derived that

$$\begin{aligned} l_r = \frac{l_\alpha}{\gamma} = \frac{z_\alpha \sigma(\hat{\gamma}_n)}{\gamma} &= \frac{z_\alpha \sqrt{E_{f^*}(\hat{\gamma}_n^2) - E_{f^*}^2(\hat{\gamma}_n)}}{\gamma\sqrt{n}} \\ &= \frac{z_\alpha \sqrt{E_{f^*}\left(I_{\mathcal{E}}^2(\boldsymbol{x})\, L^2(\boldsymbol{x})\right) - \gamma^2}}{\gamma\sqrt{n}} \\ &= \frac{z_\alpha}{\sqrt{n}} \sqrt{\frac{E_{f^*}\left(I_{\mathcal{E}}^2(\boldsymbol{x})\, L^2(\boldsymbol{x})\right)}{\gamma^2} - 1} \le \beta \end{aligned} \tag{15}$$

The required minimum test number is then

$$n \ge \frac{z_\alpha^2}{\beta^2} \left(\frac{E_{f^*}\left(I_E^2(\boldsymbol{x})\, L^2(\boldsymbol{x})\right)}{\gamma^2} - 1 \right) \tag{16}$$

When $f^*(x)$ is properly chosen, $E_{f^*}\left(I_{\mathcal{E}}^2(\boldsymbol{x})\, L^2(\boldsymbol{x})\right)$ can be close to γ^2, resulting in a smaller number of tests (i.e., the test is accelerated).

Accelerated evaluation in lane change scenarios

When a slower lane changing vehicle cut-in in front of the AV, the events of interest are defined as

$$\mathcal{E} = \{\min(R_L(t) | t_{LC} \le t \le t_{LC} + T_{LC}) \le \mathrm{R}_{\mathcal{E}}\} \tag{17}$$

where T_{LC} represents duration of the lane change event; $\mathrm{R}_{\mathcal{E}}$ is the critical range. Eq. (17) means that if the minimum range is smaller than $\mathrm{R}_{\mathcal{E}}$ anytime during the lane change event, it is declared as a event of interest.

The random vector $\boldsymbol{x}$ consists of three variables $[v_L, TTC_L^{-1}, R_L^{-1}]$. v_L is generated using empirical distributions shown in Fig. 3 directly. The IS approach considers the modified probability density functions of TTC_L^{-1} and R_L^{-1} denoted by $f^*_{TTC_L^{-1}}(\boldsymbol{x})$ and $f^*_{R_L^{-1}}(\boldsymbol{x})$. The likelihood ratio is then

$$L(R_L^{-1} = x, TTC_L^{-1} = y) = \frac{f_{R_L^{-1}}(x) f_{TTC_L^{-1}}(y)}{f^*_{R_L^{-1}}(x) f^*_{TTC_L^{-1}}(y)} \tag{18}$$

From (9), the probability of $\mathcal{E}$ can be estimated as

$$\mathrm{P}(\mathcal{E}) = \mathrm{E}_f\big(I_{\mathcal{E}}(\boldsymbol{x})\big) = \mathrm{E}_{f^*}\big(I_{\mathcal{E}}(\boldsymbol{x}) L(\boldsymbol{x})\big) \tag{19}$$

There are many possible choices for the family of altered probability density function. Here we use a class of family named the Exponential Change of Measure (ECM) for TTC_L^{-1}.

Recall that $TTC_L^{-1} \sim \exp(\lambda_{TTC_L^{-1}}(v_L))$, i.e.

$$f_{TTC_L^{-1}}(x) = \lambda_{TTC_L^{-1}} \exp(-\lambda_{TTC_L^{-1}} \cdot x) \quad (20)$$

ECM considers the family

$$f^*_{TTC_L^{-1}}(x) = \exp\left(\vartheta_{TTC_L^{-1}} x - \Psi\left(\vartheta_{TTC_L^{-1}}\right)\right) f_{TTC_L^{-1}}(x) \quad (21)$$

parametrized by $\vartheta_{TTC_L^{-1}}$, where $\Psi\left(\vartheta_{TTC_L^{-1}}\right)$ is the logarithmic moment generation function of TTC_L^{-1}, i.e.,

$$\Psi\left(\vartheta_{TTC_L^{-1}}\right) = \log \mathrm{E}\left(\exp\left(\vartheta_{TTC_L^{-1}} TTC_L^{-1}\right)\right) \quad (22)$$

It can be further shown that

$$f^*_{TTC_L^{-1}}(x) = \left(\lambda_{TTC_L^{-1}} - \vartheta_{TTC_L^{-1}}\right) \exp\left(-\left(\lambda_{TTC_L^{-1}} - \vartheta_{TTC_L^{-1}}\right) x\right) \quad (23)$$

Nominally R_L^{-1} follows a Pareto distribution, i.e.

$$f_{R_L^{-1}}(x) = Pareto\left(x \middle| k_{R_L^{-1}}, \sigma_{R_L^{-1}}, \theta_{R_L^{-1}}\right) \quad (24)$$

The ECM cannot be directly applied to a Pareto distribution directly. We first construct an exponential distribution

$$\tilde{f}_{R_L^{-1}}(x) = \lambda_{R_L^{-1}} \exp\left(-\lambda_{R_L^{-1}} x\right) \quad (25)$$

with $\lambda_{R_L^{-1}}$, which was optimized to make (25) to have the smallest least square error to (24). Then we apply ECM to (25)

$$f^*_{R_L^{-1}}(x) = \left(\lambda_{R_L^{-1}} - \vartheta_{R_L^{-1}}\right) \exp\left(-\left(\lambda_{R_L^{-1}} - \vartheta_{R_L^{-1}}\right) x\right) \quad (26)$$

$\vartheta_{R_L^{-1}}$ and $\vartheta_{TTC_L^{-1}}$ were chosen to make $P(\mathcal{E})$ converge fast. Different parameters were applied in low, medium and high velocity conditions. The parameters we used were shown in Table I.

TABLE I
$\vartheta_{R_L^{-1}}$ AND $\vartheta_{TTC_L^{-1}}$ VALUES

v_L	$5-15\ [m/s]$	$15-25\ [m/s]$	$25-35\ [m/s]$
$\vartheta_{R_L^{-1}}$	-0.1	-0.1	-0.1
$\vartheta_{TTC_L^{-1}}$	-0.5	-1	-1.5

Now the probability of $\mathcal{E}$ can be estimated by using (11) with L in (18) and modified distributions in (23) and (25).

SIMULATION ANALYSIS

The AV is assumed to be equipped with both Adaptive Cruise Control (ACC) and Autonomous Emergency Braking (AEB). When the driving is perceived to be safe ($TTC \geq TTC_{AEB}$), it is controlled by ACC. The ACC is approximated by a PI controller to achieve a desired time headway $T^{ACC}_{HW_d}$

$$t^{Err}_{HW} = t_{HW} - T^{ACC}_{HW_d} \quad (27)$$

$$a_d(t+\tau) = K_p^{ACC} t^{Err}_{HW}(t) + K_i^{ACC} \int_0^t t^{Err}_{HW}(\tau)\, d\tau \quad (28)$$

where t_{HW} is the time headway, defined as

$$t_{HW} = R_L/v \quad (29)$$

a_d is the acceleration command; gains K_p^{ACC} and K_i^{ACC} are calculated using the Matlab Control Toolbox using the following requirements: a) Loop bandwidth = 10 rad/s, and b) Phase margin = 60 degree. The ACC control is saturated at $|a_d| < a^{Max}_{ACC}$.

The AEB model was extracted from a 2011 Volvo V60, based on a test conducted by ADAC (Allgemeiner Deutscher Automobil-Club e.V.) [52] and its analysis from [53] using test track data, data found in owner's manuals, European New Car Assessment Program (Euro NCAP) information, and videos during vehicle operation. The AEB algorithm becomes active when $TTC < TTC_{AEB}$, where TTC_{AEB} depends on vehicle speed as shown in Fig. 9. Once triggered, AEB aims to achieve acceleration aAEB. In [53] aAEB was assumed to be -10 m/s2 on high friction roads. The build-up of deceleration is subject to a rate limit rAEB = -16 m/s3 as shown in Fig. 10. It should be noted that the AEB modeled here is an approximation but not necessarily a good representation of the actual system on production vehicles.

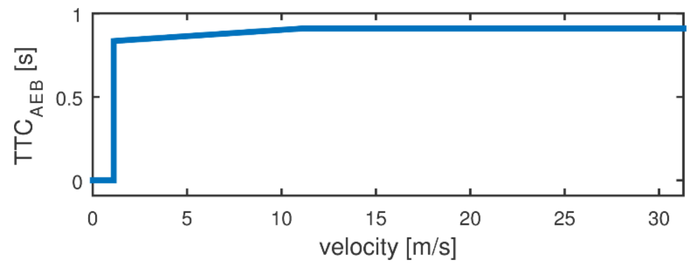

Fig. 9. TTC_{AEB} as a function of vehicle speed

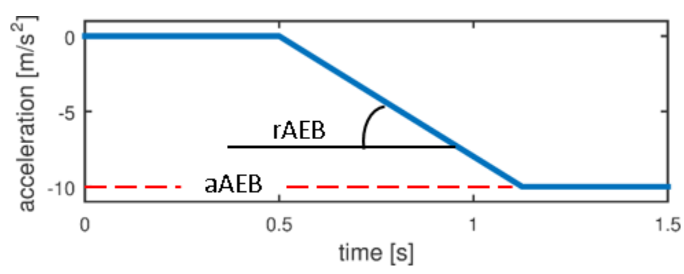

Fig. 10. The modeled AEB algorithm

To accurately model the dynamics of AV, many subsystems need to be considered, such as the engine, transmission, braking, aerodynamics, ABS (Anti-lock Braking System), etc. For simplicity, a first order lag with a time constant τ_{AV} is used to model the transfer function from the commanded acceleration to the actual acceleration. The accelerated evaluation process can be applied on other vehicle models such as CarSim if more accurate simulations are desired.

The crash event $\mathcal{E}_c$ is occurred as R_L becomes negative within T_{LC} time after t_{LC}, from (17),

$$\mathcal{E}_c = \{\mathcal{E} | \mathrm{R}_{\mathcal{E}} = 0\} \quad (30)$$

To estimate $P(\mathcal{E}_c)$, both accelerated and naturalistic simulations were conducted. Simulation parameters are shown in Table II.

TABLE II
PARAMETERS FOR THE LANE CHANGE SIMULATIONS

Variable	$T_{HW_d}^{ACC}$	a_{ACC}^{Max}	τ_{AV}	$a_L(t_{LC})$	$a(t_{LC})$	T_{LC}	Road friction
Unit	s	m/s^2	s	m/s^2	m/s^2	s	-
Value	2	5	0.0796	0	0	8	1

The crash rate is calculated after each simulation and the results are shown in Fig. 11. The naturalistic tests and accelerated tests were plotted on different scales. It can be seen that the accelerated evaluation successfully estimates the crash rate of the naturalistic conditions.

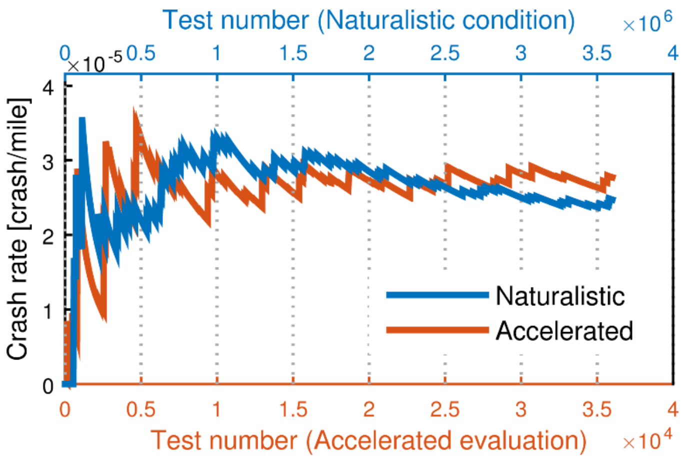

Fig. 11. Convergence of the estimation of lane change crash rate

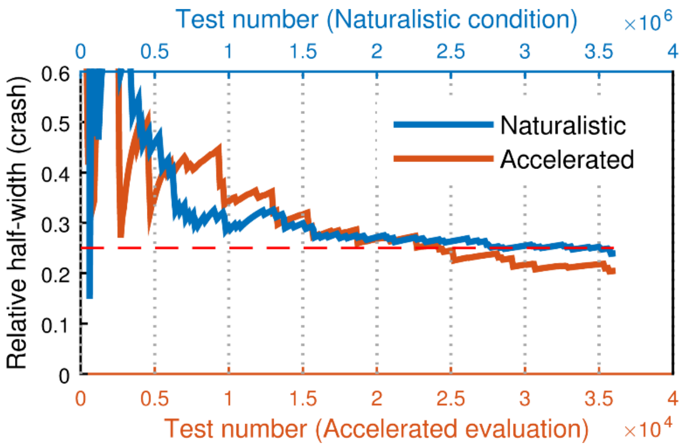

Fig. 12. Relative half width of crash events

Relative half-width is used as the criteria for convergence. The evaluation stops when the relative half-width of the estimation is below $\beta = 0.25$. Fig. 12 shows that the accelerated evaluation achieves this threshold level after 24,101 simulations, 145 times faster than the naturalistic simulations.

CONCLUSION

This paper proposes an approach to evaluate the performance of AVs in an accelerated fashion. By modifying the stochastic behaviors of the primary other vehicle (POV), in this case a lane changing vehicle driving at a slower speed than the host vehicle (the AV), higher-risk driving behaviors are sampled more frequently. This method is based on the importance sampling theories and have been developed to ensure unbiased and accurate evaluation under accelerated conditions. Simulation results show that the proposed method accelerates the evaluation procedure by about 145 times. Possible future work includes achieve high acceleration ratio, extending the methodology to dynamic driving conditions, and a more systematic way to select the modified probability density function for unbiased results.

ACKNOWLEDGMENTS

The authors would like to acknowledge the generous sponsorship of the National Institute for Occupational Safety and Health (NIOSH).

DISCLAIMERS

The findings and conclusions in the report are those of the author(s) and do not necessarily represent the views of the National Institute for Occupational Safety and Health (NIOSH). Mention of company names or products does not imply endorsement by NIOSH.

REFERENCES

[1] C. Lewis, "The Economic Benefits of Driverless Cars," *Morgan Stanley*, 2014. [Online]. Available: http://robotenomics.com/2014/02/26/morgan-stanley-the-economic-benefits-of-driverless-cars/. [Accessed: 22-Aug-2014].

[2] C. Laslau, "Set Autopilot for Profits: Capitalizing on the $87 Billion Self-Driving Car Opportunity," Lux Research, 2014.

[3] J. Treat, N. Tumbas, and S. McDonald, "Tri-level study of the causes of traffic accidents: final report," DOT HS 034 3 535, 1979.

[4] L. Blincoe, T. R. Miller, E. Zaloshnja, and B. A. Lawrence, "The Economic and Societal Impact Of Motor Vehicle Crashes, 2010 (Revised)," NHTSA, DOT HS 812 013, 2015.

[5] FESTA-Consortium, "FESTA Handbook Version 2 Deliverable T6.4 of the Field opErational teSt supporT Action," Brussels: European Commission, 2008.

[6] M. Aust, "Evaluation Process for Active Safety Functions: Addressing Key Challenges in Functional, Formative

Evaluation of Advanced Driver Assistance Systems," Chalmers University of Technology, 2012.
[7] D. LeBlanc, J. Sayer, C. Winkler, R. Ervin, S. Bogard, M. Devonshire, J. Mefford, M. Hagan, Z. Bareket, R. Goodsell, and T. Gordon, "Road Departure Crash Warning System Field Operational Test : Methodology and Results," UMTRI-2006-9-2, 2006.
[8] M. Perez, L. S. Angell, J. Hankey, R. K. Deering, R. E. Llaneras, C. A. Green, M. L. Neurauter, and J. F. Antin, "Advanced Crash Avoidance Technologies (ACAT) Program – Final Report of the GM-VTTI Backing Crash Countermeasures Project," DOT HS 811 452, 2011.
[9] T. Victor, J. Bärgman, M. Hjälmdahl, and K. Kircher, "Sweden-Michigan Naturalistic Field Operational Test (SeMiFOT) Phase 1 : Final Report," 2010.
[10] J. Sayer, D. LeBlanc, S. Bogard, D. Funkhouser, F. Operational, T. Final, and P. Report, "Integrated Vehicle-Based Safety Systems Field Operational Test Final Program Report," NHTSA, DOT HS 811 482, 2011.
[11] T. Gordon, H. Sardar, D. Blower, M. Ljung Aust, Z. Bareket, M. Barnes, A. Blankespoor, I. Isaksson- Hellman, J. Ivarsson, B. Juhas, K. Nobukawa, and H. Theander, "Advanced Crash Avoidance Technologies (ACAT) Program – Final Report of the Volvo-Ford- UMTRI Project : Safety Impact Methodology for Lane Departure Warning – Method Development And Estimation of Benefits," DOT HS 811 405, 2010.
[12] Wikipedia, "Google driverless car." [Online]. Available: http://en.wikipedia.org/wiki/Google_driverless_car.
[13] C. Kessler and A. Etemad, "Deliverable D11.3 Final Report."
[14] J. S. Hickman and R. J. Hanowski, "An assessment of commercial motor vehicle driver distraction using naturalistic driving data.," *Traffic Inj. Prev.*, vol. 13, no. 6, pp. 612–9, 2012.
[15] T. A. Dingus, S. G. Klauer, V. L. Neale, A. Petersen, S. E. Lee, J. Sudweeks, M. A. Perez, J. Hankey, D. Ramsey, S. Gupta, C. Bucher, Z. R. Doerzaph, J. Jermeland, and R. . Knipling, "The 100-Car Naturalistic Driving Study Phase II – Results of the 100-Car Field Experiment," NHTSA, DOT HS 810 593, 2006.
[16] NHTSA, "Traffic Safety Facts 2012," 2012.
[17] M. Akamatsu, P. Green, and K. Bengler, "Automotive technology and human factors research: Past, present, and future," *Int. J. Veh. Technol.*, vol. 2013, pp. 1–27, 2013.
[18] H.-H. Yang and H. Peng, "Development and evaluation of collision warning/collision avoidance algorithms using an errable driver model," *Veh. Syst. Dyn.*, vol. 48, no. sup1, pp. 525–535, Dec. 2010.
[19] K. Lee, "Longitudinal driver model and collision warning and avoidance algorithms based on human driving databases," University of Michigan., 2004.
[20] Euro NCAP, "Euro NCAP test protocol – AEB systems," 2013.
[21] K. Deering, Richard, "Crash Avoidance Metrics Partnership Annual Report, April 2001 - March 2002," DOT HS 809 531, 2002.
[22] O. Carsten, N. Merat, W. H. Janssen, E. Johansson, M. Fowkes, and K. A. Brookhuis, "Human Machine Interaction and the Safety of Traffic in Europe Final Report," 2005.
[23] H. Kussmann, H. Modler, J. Engstrom, A. Agnvall, P. Piamonte, G. Markkula's, A. Amditis, A. Bolovinou, L. Andreone, E. Deregibus, and P. Kompfner, "Requirements for AIDE HMI and safety functions," D3.2.1, 2004.
[24] V. Karabatsou, M. Pappas, P. van Elslande, K. Fouquet, and M. Stanzel, "A-priori evaluation of safety functions effectiveness - Methodologies Table of Contents," D4.1.3, 2007.
[25] T. Wohllebe, J. Vetter, C. Mayer, M. McCarthy, and R. de Lange, "Integrated Project on Advanced Protection Systems," AP-SP13-0035 Project, 2004.
[26] J.-A. Bühne, A. Lüdeke, S. Schönebeck, J. Dobberstein, H. Fagerlind, A. Bálint, and M. McCarthy, "Assessment of Integrated Vehicle Safety Systems for improved vehicle," ASSESS D2.2 (2/2) Socio-economic, 2012.
[27] W. G. Najm and J. D. Smith, "Development of Crash Imminent Test Scenarios for Integrated Vehicle-Based Safety Systems," DOT HS 810 757, 2007.
[28] "NASS General Estimates System | National Highway Traffic Safety Administration (NHTSA)." [Online]. Available: http://www.nhtsa.gov/Data/National+Automotive+Sampling+System+(NASS)/NASS+General+Estimates+System. [Accessed: 04-Sep-2014].
[29] "NCSA Publications & Data Requests." [Online]. Available: http://www-nrd.nhtsa.dot.gov/Cats/listpublications.aspx?Id=227&ShowBy=Category. [Accessed: 04-Sep-2014].
[30] "Event Data Recorder (EDR) | National Highway Traffic Safety Administration (NHTSA)." [Online]. Available: http://www.nhtsa.gov/EDR. [Accessed: 04-Sep-2014].
[31] D. LeBlanc, M. Gilbert, S. Stachowski, and R. Sherony, "Tradeoffs in the Evaluation of Light Vehicle Pre-Collision Systems," in *SAE 2014 World Congress & Exhibition*, 2014.
[32] H. Peng and D. Leblanc, "Evaluation of the performance and safety of automated vehicles," *White Pap. NSF Transp. CPS Work.*, 2012.
[33] W.-H. Ma and H. Peng, "A Worst-Case Evaluation Method for Dynamic Systems," *J. Dyn. Syst. Meas. Control*, vol. 121, no. 2, p. 191, 1999.
[34] A. Ungoren and H. Peng, "An adaptive lateral preview driver model," *Veh. Syst. Dyn.*, vol. 43, no. 4, pp. 245–259, Apr. 2005.
[35] Y. Kou, "Development and evaluation of integrated chassis control systems," The University of Michigan, 2010.
[36] Y. Fujii and R. Shiobara, "The Analysis of Traffic Accidents," *J. Navig.*, vol. 24, no. 04, p. 534, Jan. 2010.

[37] F. Goerlandt and P. Kujala, “Traffic simulation based ship collision probability modeling,” *Reliab. Eng. Syst. Saf.*, vol. 96, no. 1, pp. 91–107, Jan. 2011.
[38] D. Zhao, H. Peng, S. Bao, K. Nobukawa, D. J. LeBlanc, and C. S. Pan, “Accelerated evaluation of automated vehicles using extracted naturalistic driving data,” in *Proceeding for 24th International Symposium of Vehicles on Road and Tracks*, 2015.
[39] G. M. Fitch, S. E. Lee, S. Klauer, J. Hankey, J. Sudweeks, and T. Dingus, “Analysis of Lane-Change Crashes and near-Crashes,” *US Dep. Transp. Natl. Highw. Traffic Saf. Adm.*, 2009.
[40] S. E. Lee, C. B. E. Olsen, W. W. Wierwille, NHTSA, and D. O. T. Hs, “A Comprehensive Examination of Naturalistic Lane-Changes,” no. March, 2004.
[41] D. Zhao, H. Peng, K. Nobukawa, S. Bao, D. J. LeBlanc, and C. S. Pan, “Analysis of Mandatory and Discretionary Lane Change Behaviors for Heavy Trucks,” in *12th International Symposium on Advanced Vehciel Control*, 2014.
[42] D. LeBlanc, “Data from the Safety Pilot Model Deployment.” [Online]. Available: http://assets.conferencespot.org/fileserver/file/46778/filename/39ftvo.pdf. [Accessed: 22-Aug-2014].
[43] J. Harding, G. Powell, R. Yoon, and J. Fikentscher, “Vehicle-to-vehicle communications: Readiness of v2v technology for application,” 2014.
[44] P. Heidelberger, “Fast simulation of rare events in queueing and reliability models,” *ACM Trans. Model. Comput. Simul.*, vol. 5, no. 1, pp. 43–85, Jan. 1995.
[45] P. Glasserman and J. Li, “Importance Sampling for Portfolio Credit Risk,” *Manage. Sci.*, Nov. 2005.
[46] S. Asmussen and H. Albrecher, *Ruin probabilities*, 2nd ed. World Scientific, 2010.
[47] C.-S. Chang, P. Heidelberger, S. Juneja, and P. Shahabuddin, “Effective bandwidth and fast simulation of ATM intree networks,” *Perform. Eval.*, vol. 20, no. 1–3, pp. 45–65, May 1994.
[48] J. Bucklew, *Introduction to rare event simulation*. Springer Science & Business Media, 2013.
[49] J. Blanchet and H. Lam, “State-dependent importance sampling for rare-event simulation: An overview and recent advances,” *Surv. Oper. Res. Manag. Sci.*, vol. 17, pp. 38–59, 2012.
[50] S. Juneja and P. Shahabuddin, “Chapter 11 Rare-Event Simulation Techniques: An Introduction and Recent Advances,” *Handbooks Oper. Res. Manag. Sci.*, vol. 13, no. 06, pp. 291–350, 2006.
[51] H. L. Royden, *Real Analysis*. New York: Prentice Hall, 1948.
[52] ADAC, “Comparative test of advanced emergency braking systems,” 2011.
[53] T. I. Gorman, “Prospects for the collision-free car : The effectiveness of five competing forward collision avoidance systems,” Virginia Polytechnic Institute and State University, 2013.